

## Reduction in dark current using resonant tunneling barriers in quantum dots-in-a-well long wavelength infrared photodetector

A. V. Barve,<sup>1</sup> S. Y. Shah,<sup>2</sup> J. Shao,<sup>1</sup> T. E. Vandervelde,<sup>1</sup> R. V. Shenoi,<sup>1</sup> W.-Y. Jang,<sup>1</sup> and S. Krishna<sup>1,a)</sup>

<sup>1</sup>Center for High Technology Materials, Department of Electrical and Computer Engineering, University of New Mexico, Albuquerque, New Mexico 87106, USA

<sup>2</sup>Department of Electrical Engineering, Indian Institute of Technology Bombay, Mumbai 400076, India

(Received 25 July 2008; accepted 17 September 2008; published online 3 October 2008)

We report the use of resonant tunneling (RT) assisted barriers to reduce the dark current in quantum dots-in-a-well (DWELL) infrared photodetectors. Designed RT barriers allow energy-selective extraction of photoexcited carriers while blocking a continuum of energies. Over two orders of magnitude reduction in the dark current in the RT-DWELL device over a control sample without RT-DWELL at 77 K has been demonstrated. Specific detectivity ( $D^*$ ) of  $3.6 \times 10^9 \text{ cm Hz}^{1/2} \text{ W}^{-1}$  at 77 K at  $\lambda_{\text{peak}} = 11 \mu\text{m}$  with a conversion efficiency of 5.3% was obtained in the RT-DWELL device.  $D^*$  for the RT-DWELL device is five times higher than that of the control sample. © 2008 American Institute of Physics. [DOI: 10.1063/1.2996410]

Quantum dot intersubband photodetectors (QDIP) are being widely researched<sup>1,2</sup> as an emerging technology for low-volume high-performance infrared detectors. The competing technologies in today's market are mercury-cadmium-telluride based detectors,<sup>3</sup> quantum well intersubband photodetectors,<sup>4</sup> and strained-layer superlattice based detectors.<sup>5</sup> QDIPs promise low dark currents, higher operating temperature, large area uniformity.<sup>6</sup> Reduction in the dark current is possible because of the three dimensional confinement of carriers inside a QD.

The quantum dots-in-a-well (DWELL) detectors,<sup>7-11</sup> in which QDs are placed inside a single or double quantum well, has been a topic of extensive research in several research groups for the past few years. DWELL based detectors combine the advantages of QDIPs, such as three-dimensional confinement, with the added advantages such as ease of controlling the peak wavelength with repeatable, dial-in type growth recipes and bias tunable spectral response.<sup>12</sup> The design of typical DWELL detectors involves a trade-off between lower dark current and higher peak wavelength. Typical dark current blocking layers, which offer triangular barriers, also block the photocurrent at higher wavelengths. We propose the use of resonant tunneling (RT) barriers for DWELL detectors, which remove the trade-off by a clever barrier design, as they allow the carriers within a certain energy band to pass through, while blocking a continuum of energies, thereby reducing the dark current. RT barriers have been previously employed to reduce the dark current in QDIPs.<sup>13</sup> In this paper, we report the use of RT barriers in a DWELL design. Over three orders of magnitude reduction in the dark current has been demonstrated. The specific detectivity for the RT-DWELL sample is  $3.6 \times 10^9 \text{ cm Hz}^{1/2} \text{ W}^{-1}$  at 77 K at  $-1.1 \text{ V}$  bias, a factor of 5 improvement over a control sample. Conversion efficiency was 5.3% at this bias for RT-DWELL device for  $\lambda_{\text{peak}} = 11 \mu\text{m}$ .

The samples were grown in a V-80 molecular beam epitaxy system. The RT-DWELL sample has ten stacks of InAs QDs in a 7.5 nm  $\text{In}_{0.15}\text{Ga}_{0.85}\text{As}$  quantum well. The RT barrier on the top of the DWELL in each stack has 2 nm GaAs, 2 nm  $\text{Al}_{0.3}\text{Ga}_{0.7}\text{As}$ , 5.5 nm  $\text{In}_{0.15}\text{Ga}_{0.85}\text{As}$ , and 2 nm  $\text{Al}_{0.3}\text{Ga}_{0.7}\text{As}$ . There is an additional 50 nm GaAs barrier between the stacks. The control sample has the same structure without the RT-barrier. The RT-barrier was designed to allow the photocarriers, excited from the dot, in forward bias, to be extracted through RT. Forward bias is defined as positive voltage applied to the top contact. Since the passband of RT barrier is aligned with the conduction band edge of GaAs, it also allows the thermalized carriers to pass through in the negative bias. The calculated band diagram, energy eigenvalues, and wavefunctions are shown in Fig. 1. Calculated tunneling probability as a function of energy for an uncoupled RT-barrier is shown in the inset. Three point finite difference method was used to simulate the coupled well and RT-barrier structure,<sup>14</sup> while the transfer matrix method<sup>15</sup> was used to calculate the tunneling probability for RT-barriers. Results from both methods are in excellent agreement (within 2%).

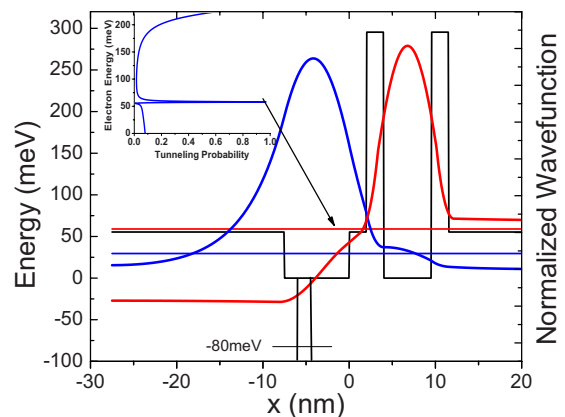


FIG. 1. (Color online) Calculated eigenenergies and wavefunctions in RT-DWELL QDIP. The resonance passband is aligned to the conduction band of GaAs. Inset shows a sharp tunneling probability peak at this energy ( $\sim 57 \text{ meV}$ ). QD location has been shown for reference.

<sup>a)</sup>Tel.: (505) 272 7800. FAX: (505) 272 7801. Electronic mail: skrishna@chtm.unm.edu.

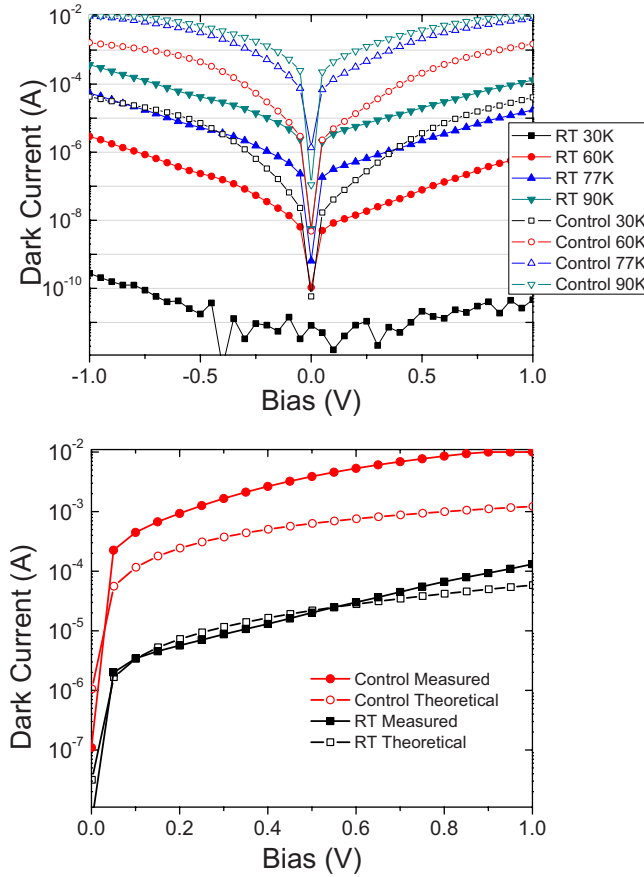


FIG. 2. (Color online) (a) Measured dark current for RT-DWELL (filled symbols) and a control sample (hollow symbols)  $400 \times 400 \mu\text{m}^2$  mesa device. (b) Comparison of the theoretically predicted dark current with the measured dark current values for the two devices at 90 K.

with each other, for the calculations of wavefunctions and energy eigenvalues. It is to be noted that the mentioned calculations simulate only two-dimensional wavefunctions, ignoring the presence of the QD, since only thermally excited carriers are expected to dominate the dark current. A detailed Green's function based modeling can be found in Naser *et al.*<sup>16</sup> As seen in the inset, the RT-barriers have a sharp transmission peak at the resonance energy, with negligible transmission for carriers with other energies. This leads to a lower dark current, without affecting the operating wavelength.

The dark current in a DWELL device can be approximately modeled by a simplistic model based on the calculation of tunneling probability for the carriers from the QD through the barriers.<sup>13</sup> Surface dot density of  $5 \times 10^{10} \text{ cm}^{-2}$ , inhomogeneous broadening of 40 meV, saturation velocity of  $2 \times 10^7 \text{ cm/s}$ , and electron mobility of  $1000 \text{ cm}^2/\text{V s}$  were assumed for the calculations. Fermi level was assumed to be located just above the ground state of the dot, as the dots are doped at approximately one electron per dot. Figure 2(a) shows the measured dark currents for the two samples. As seen from the figure, three to four orders of magnitude improvement in the measured dark current in RT-DWELL samples at low temperatures is apparent as compared to the control sample. As the temperature increases, the improvement factor decreases to one to two orders of magnitude, but is still very significant. Figure 2(b) shows the comparison of the theoretically predicted dark current with the measured

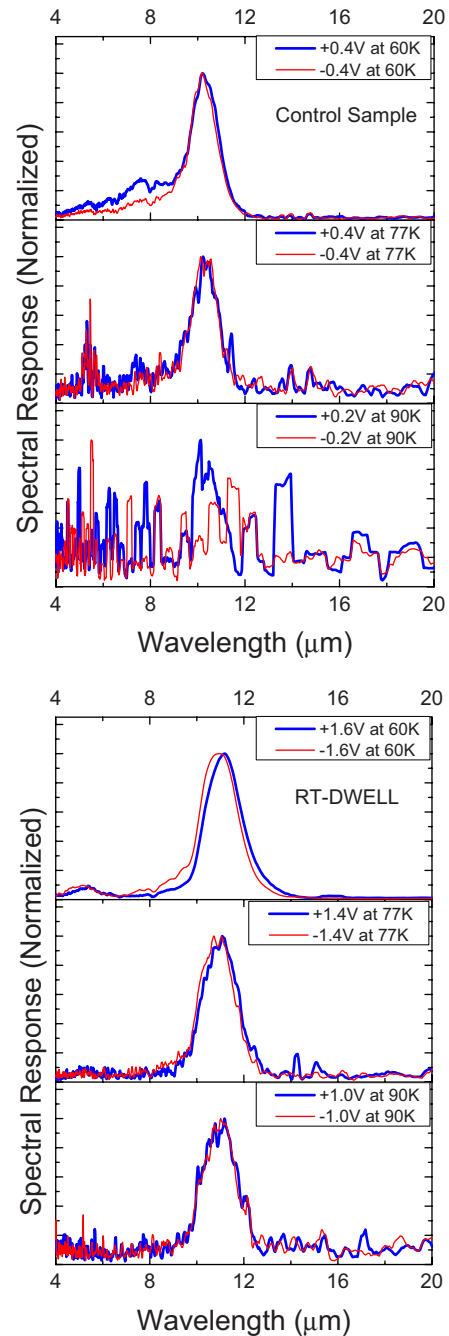


FIG. 3. (Color online) Normalized spectral response of (a) Control sample (b) RT-DWELL sample at 30, 60, and 90 K. Note that at 90 K and at the maximum operating bias of the device, the spectral response from the RT-DWELL is much stronger than that of the control sample.

dark current for the two devices at 90 K. It can be seen that although the results match well for RT-DWELL devices, the measured dark current is actually higher than that predicted theoretically in the control sample. This is presumably because of the simplicity of the model, which ignores thermionic emission from the ground state of QD. A practical consequence of reduction in the dark current is the increase in the operating bias range. This plays an important role in compensating for the loss of signal due to resonant RT, as seen later.

The reduction in the dark current is directly mapped into improvement in the operating temperature and the operating bias range of the device, as seen from Fig. 3. The normalized spectral response comparison at different temperatures shows

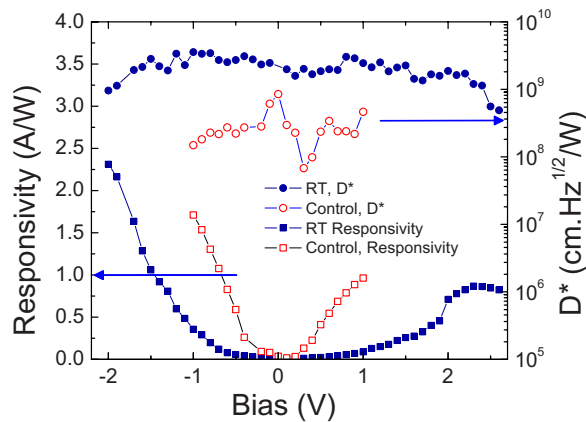


FIG. 4. (Color online) Comparison of the measured responsivity (squares) and  $D^*$  (circles) for the two devices at 77 K.

the improvement in the signal-to-noise ratio. It is important to compare devices with similar peak wavelength for a fair comparison, as the dark current increases exponentially with the response wavelength. Suppression of  $6\text{--}9\ \mu\text{m}$  response in RT-DWELL samples proves the existence of narrow pass-band resonance level, which allows passage of only a designed long-wavelength peak, which is believed to be originating from a bound to bound transition from QD to quantum well, as depicted in Fig 1. A low pass filter was used to remove spurious noisy peaks in the response.

Even though RT barriers decrease the dark current, they also decrease the photocurrent, thereby decreasing the responsivity. Figure 4 shows the comparison of responsivity and specific detectivity of the two samples at 77 K. Responsivity and  $D^*$  were measured at 77 K using a pour-fill dewar and a 900 K blackbody source. The substrate scattering effects were neglected while calculating the responsivity. The responsivity is reduced by a factor of 2–5 at a given voltage. However, due to the larger operating bias range, the measured peak responsivity for RT-DWELL is actually higher than that of the control sample. Secondly, since the rms noise current is also reduced, the reduction in the responsivity at a particular bias is more than compensated such that there is a net improvement in the signal to noise ratio, resulting in factor of 5 improvement in  $D^*$ . The negative bias shows a relatively higher responsivity, as the carriers are thermalized before reaching the RT-barriers, and hence can pass through as the pass-band is designed to be very close to the GaAs conduction band.

It should be noted that a simple device structure was used as a proof of concept for a RT-DWELL device and related theoretical calculations. A significant improvement in

the device performance can be expected by the use of better designs for the parent sample, such as a double well structure, which reduces the cumulative compressive strain per stack,<sup>17</sup> allowing more number of stacks, thereby increasing the responsivity.

In conclusion, we present the design and characterization of a RT barrier based DWELL samples. Two to four orders of magnitude improvement in the dark current of the device has been demonstrated for this device over a control sample. Careful analysis of spectral response clearly demonstrates the effect of RT in these devices. Peak specific detectivity of  $\sim 3.6 \times 10^9\ \text{cm Hz}^{1/2}\ \text{W}^{-1}$  at 77 K, at a peak wavelength of  $11\ \mu\text{m}$ , for RT-DWELL device shows a factor of 5 improvement over the control sample, in this unoptimized structure. Reduction in responsivity can be compensated by a larger operating bias range, which is a direct consequence of the reduction in the dark current by RT barriers. The peak responsivity is 2.3 A/W at  $-2\ \text{V}$  bias at 77 K, which gives conversion efficiency of 26%.

Work supported by AFRL, NSF, AFOSR, IC Postdoc Program and KRIS-GRL Program.

- <sup>1</sup>S. Maimon, E. Finkman, G. Bahir, S. E. Schacham, J. M. Garcia, and P. M. Petroff, *Appl. Phys. Lett.* **73**, 2003 (1998).
- <sup>2</sup>S. Raghavan, P. Rotella, A. Stintz, B. Fuchs, S. Krishna, C. Morath, D. A. Cardimona, and S. W. Kennerly, *Appl. Phys. Lett.* **81**, 1369 (2002).
- <sup>3</sup>A. Rogalski, *Rep. Prog. Phys.* **68**, 2267 (2005).
- <sup>4</sup>J. L. Pan and C. G. Fonstad, *Mater. Sci. Eng., R.* **28**, 65 (2000).
- <sup>5</sup>A. Rogalski and P. Martyniuk, *Infrared Phys. Technol.* **48**, 39 (2006).
- <sup>6</sup>S. D. Gunapala, S. V. Bandara, C. J. Hill, D. Z. Ting, J. K. Liu, S. B. Rafol, E. R. Blazejewski, J. M. Mumolo, S. A. Keo, S. Krishna, Y. C. Chang, and C. A. Shott, *IEEE J. Quantum Electron.* **43**, 203 (2007).
- <sup>7</sup>S. Krishna, *J. Phys. D: Appl. Phys.* **38**, 2142 (2005).
- <sup>8</sup>S. Krishna, S. Gunapala, S. V. Bandara, C. Hill, and D. Z. Ting, *Proc. IEEE* **95**, 1838 (2007).
- <sup>9</sup>G. Jolley, L. Fu, H. H. Tan, and C. Jagadish, *Appl. Phys. Lett.* **92**, 193507 (2008).
- <sup>10</sup>H. Lim, S. Tsao, W. Zhang, and M. Razeghi, *Appl. Phys. Lett.* **90**, 131112 (2007).
- <sup>11</sup>T. E. Vandervelde, M. C. Lenz II, E. Varley, A. Barve, J. Shao, R. Sheno, D. A. Ramirez, W. Jang, Y. Sharma, and S. Krishna, *Proc. SPIE* **6940**, 694003 (2008).
- <sup>12</sup>E. Varley, M. Lenz, S. J. Lee, J. S. Brown, D. A. Ramirez, A. Stintz, S. Krishna, A. Reisinger, and M. Sundaram, *Appl. Phys. Lett.* **91**, 081120 (2007).
- <sup>13</sup>X. Su, S. Chakrabarti, P. Bhattacharya, G. Ariyawansa, and A. G. Unil Perera, *IEEE J. Quantum Electron.* **49**, 974 (2005).
- <sup>14</sup>I. H. Tan, G. Snider, L. Chang, and E. Hu, *J. Appl. Phys.* **68**, 4071 (1990).
- <sup>15</sup>R. Tsu and L. Esaki, *Appl. Phys. Lett.* **22**, 562 (1973).
- <sup>16</sup>M. A. Naser, M. J. Deen, and D. A. Thompson, *J. Appl. Phys.* **102**, 083108 (2007).
- <sup>17</sup>R. V. Sheno, R. S. Attaluri, A. Siroya, J. Shao, Y. D. Sharma, A. Stintz, T. E. Vandervelde, and S. Krishna, *J. Vac. Sci. Technol. B* **26**, 1136 (2008).